Nucleic Acid Sequencing

DOI: 10.1002/anie.201303529

Nanopore-Based Sequencing and Detection of Nucleic Acids

*Yi-Lun Ying, Junji Zhang, Rui Gao, and Yi-Tao Long**

DNA sequencing · ion channels · membrane proteins · nanopores · single-molecule studies

Nanopore-based techniques, which mimic the functions of natural ion channels, have attracted increasing attention as unique methods for single-molecule detection. The technology allows the real-time, selective, high-throughput analysis of nucleic acids through both biological and solid-state nanopores. In this Minireview, the background and latest progress in nanopore-based sequencing and detection of nucleic acids are summarized, and light is shed on a novel platform for nanopore-based detection.

1. Introduction

Natural ion channels selectively and sophisticatedly regulate the shuttling of biomolecules, ions, protons, and even electrons through membranes, and thus are crucial for almost all cellular events. By mimicking the functions of natural ion channels, a nanopore is constructed in an impermeable membrane that separates two chambers filled with electrolyte solution. The first reported nanopore-based biosensor utilized nanopores consisting of a single α-hemolysin (αHL) with a constriction of 1.4 nm at the narrowest point.[1] Because of the appropriate inner diameter of αHL and its ability to repeatedly self-assemble, the αHL is preferentially used in the detection of biomolecules. The most efficient way to extend the application of nanopores toward sensing a wider range of biomolecules is the modification of their dimension. Hence, various biological membrane proteins, including areolysin,[2] *Mycobacterium smegmatis* porin A (MspA),[3] ClyA,[4] FhuA,[5] membrane-adapted phi29 motor protein,[6] and SP1,[7] have been used in nanopore-based sensing methods. Using microfabrication technologies, nanometer-sized apertures have been successfully drilled into thin, insulating, solid-state membranes, known as solid-state nanopores, to mimic biological nanopores. Continued efforts have enabled the integration of optical components, sophisticated electronics, and a variety of detection devices into solid-state nanopores.[8]

[*] Y.-L. Ying, Dr. J. J. Zhang, R. Gao, Prof. Y.-T. Long
Key Laboratory for Advanced Materials & Department of Chemistry, East China University of Science and Technology
130 Meilong Road, Shanghai 200237 (P. R. China)
E-mail: ytlong@ecust.edu.cn

Nanopores can be sorted into two categories, biological nanopores and solid-state nanopores, both of which have the ability to confine a molecule of interest in a nanoscale cavity. When an analyte enters a nanopore, it induces a transient change in the ion flux (current) originating from volume exclusion (Figure 1). The addition of the biomolecule to one of the electrolyte chambers generates a string of blockade currents. The properties of biomolecules, such as size, structure, conformation, and dynamic motion can be decoded by monitoring and statistically analyzing these blockade currents, their durations, and even the shapes of the blockades. The concept of mimicking ion channels enables the detection of biomolecules with nanopore-based techniques that do not require labeling, surface immobilization, or biomolecular modification. Therefore, nanopore-based techniques are powerful methods for the sensing of single molecules.[9] In particular, they constitute a promising approach for the detection of individual nucleic acids at single-

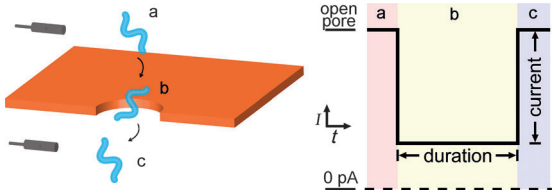

Figure 1. Model illustrating the principle of nanopore-based detection. A nucleic acid strand a) enters the nanopore, causing the abrupt decrease of the ion current from its initial open-pore current, b) passes through the cavity of the nanopore, resulting in a characteristic blockade current and duration, and c) eventually translocates through the pore, allowing the ion current to return to the open-pore state. The driving potential is applied by two electrodes. pA = pico-Ampere.

molecule level. For example, nanopore-based techniques were proposed as the candidates with the highest potential for "third-generation" DNA sequencing.[10] In an ideal nanopore-based-sequencing experiment, the nucleotides in a single-stranded DNA (ssDNA) are threaded through the pore in a strictly sequential single-file order, resulting in the local unraveling of the nucleic acid strand. In the past two decades, exciting experimental progress has been made in nanopore-based sequencing. In this Minireview, we will first focus on the progress made in single-molecule detection of nucleic acids with both biological nanopores and solid-state nanopores. Furthermore, we will shed light on the latest progress made with novel platforms for detection.

2. Biological Nanopores

2.1. DNA Sequencing with Biological Nanopores

In 1996, Kasianowicz et al. discovered that ssDNA and RNA could be driven electrophoretically through an αHL nanopore (Figure 1).[1a] Thus, nanopore-based techniques have been proposed as potential candidates for "third-generation" DNA sequencing. Though promising, some challenges need to be overcome in order to develop nanopores for DNA sequencing devices. A major hurdle of nanopore-based DNA sequencing is that the translocation of ssDNA through the pore channel is too rapid to gain information about single bases. Early results demonstrated that the translocation rate of polynucleotides is around 1–10 μs/base,[1b,11] which is beyond the temporal resolution of commercial detection devices. Therefore, controlling the speed at which DNA translocates through a pore is one of the most important challenges that need to be addressed for the development of nanopore-based sequencing.[10] To improve the time resolution, various strategies have been applied, such as increasing the viscosity of the sample solution,[12] lowering the temperature of the fluid,[13] and setting "molecular brakes" by mutagenesis.[14] One of the most efficient methods to overcome the obstacles of velocity is the use of enzymes as molecular motors to control the translocation of DNA. For example, polymerase has a turnover time in the range of tens of milliseconds per generated nucleotide while it ratchets along a DNA strand one nucleotide at a time.[15] While the enzyme processes ssDNA, the strand is pulled through the pore channel in a much slower rate of around 20 ms for bacteriophage T7 DNA polymerase and around 300 ms for the Klenow fragment of *Escherichia coli* DNA polymerase I.[16] To improve the time resolution of DNA sequencing, bacteriophage phi29 DNA polymerase (phi29 DNAP) was used in nanopores.[17] Phi29 DNAP, as a B-family polymerase, remains bound to DNA that is captured in the αHL pore about 10000 times longer than A-family polymerases.[17] Akeson and co-workers further illustrated that a DNA strand is ratcheted by phi29 DNAP in a single-file order through the pore at a rate of 2.5–40 bases/s.[18] It is also noteworthy that in a previous study this improved strategy of blocking the oligomer eliminated the active voltage control to effect polymerase binding to DNA.[19] Therefore, an automated forward and reverse ratcheting of each DNA strand through the pore was enabled for optimized and more precise DNA sequencing (Figure 2a).

Another major concern regarding nanopore-based DNA sequencing is the improvement of the current resolution, that is, the amplification of the difference between nucleotide-induced current blockade signals for the distinct and precise detection of each nucleobase. A strategy termed "sequencing by synthesis" with polymerase and coumarin-PEG-tagged

Yi-Lun Ying graduated from the East China University of Science and Technology (ECUST) in 2009. She is currently pursuing her PhD in the field of nanopore-based single-molecule studies to elucidate interactions between biomolecules and in situ nanospectroelectrochemistry in the group of Prof. Long.

Rui Gao graduated from ECUST in 2013. He is currently pursuing his PhD studies under the supervision of Prof. Long in the field of developing ultralow current amplifier and data analysis software for nanopore-based detection.

Junji Zhang received his PhD degree from ECUST in 2012 under the supervision of Prof. He Tian and is currently a lecturer at ECUST. His research interests are mainly focused on single-molecule sensing, photochromic materials, and supramolecular switches on membranes.

Yi-Tao Long received his PhD in bioelectroanalytical chemistry from Nanjing University in 1998. After completing his postdoctoral study at the University of Heidelberg, he worked as a research scientist at the Universities of Saskatchewan and Alberta and the Department of Bioengineering at UC Berkeley. Dr. Long was appointed full Professor at ECUST in 2007. His main research interests are nanopore-based single-molecule analysis, nanospectroscopy, biointerfaces/biointerphases, spectroelectrochemistry, and integrated biosensors

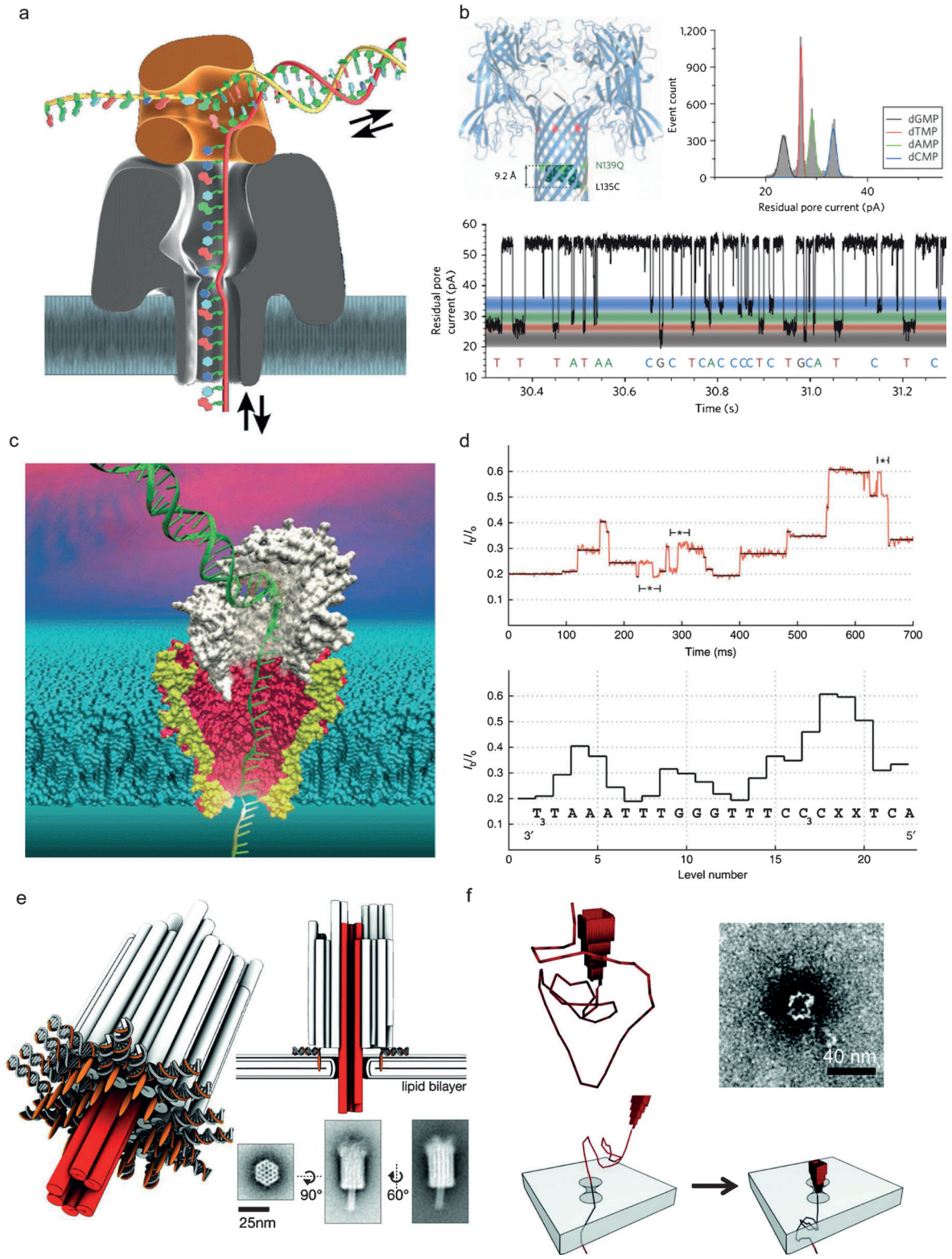

Figure 2. Strategies for DNA sequencing with biological nanopores. a) Control of the translocation speed of a DNA strand through an αHL pore (gray) by phi29 DNAP (brown).[18] b) Covalent attachment of cyclodextrin (dark blue) to the β-barrel of mutated αHL (light blue).[24] A histogram of blockade currents and current traces for the mononucleotides, produced from ssDNA and Exonuclease I, exhibits four characteristic levels corresponding to the four nucleotides, respectively. c) Integration of phi29 DNAP into mutated MspA for DNA sequencing.[3a,26] d) The real current traces (top) and the extracted mean currents illustrates sequencing of a known DNA molecule.[3a] e) A DNA origami transmembrane channel.[27] f) A DNA origami nanopore inserted into a solid-state nanopore.[28] Reproduced with permission from Ref. [3a, 18, 24, 26, 27].

nucleotides amplifies the distinction between the current for each of the four nucleobases.[20] Studies show that there are three nucleobase recognition sites located in the β-barrel of an αHL nanopore.[21] The enhanced recognition at one or two sites as well as the elimination of other sites is necessary to improve the identification of the bases by mutagenesis.[22] In order to detect each nucleobase, the αHL pores are equipped with β-cyclodextrin as a molecular adapter, because β-cyclodextrin binds mononucleotides and fits well inside the αHL channel.[23] With β-cyclodextrin covalently attached to αHL, the four nucleotides produced from ssDNA and exonuclease I were identified with excellent accuracy of around 99.8% (Figure 2b).[24]

Up until now, most nanopore-based sequencing techniques were developed with well-studied αHL because of its easy modification and reliable accuracy in the subnanometer region. However, around 20 nucleotides span the β-barrel of an αHL nanopore, which has a length of around 5.2 nm.[25] This structural limitation results in ambiguous current differential signals during the detection of the sequence, because it is difficult to determine the precise contribution of each base to the observed blockade current. To circumvent this structural drawback, *Mycobacterium smegmatis* porin A (MspA) was selected as a better candidate for nanopore-based DNA sequencing.[3b,29] It has a single constriction with a diameter of around 1.2 nm and a length of around 0.5 nm, which results in well-resolved current signals for four neighboring nucleotides. In combination with the mutated MspA and phi29 DNAP, a well-resolved and reproducible ionic current level with median durations of approximately 28 ms and current differences of up to 40 pA were observed (Figure 2c).[3a] Because of the complex current pattern and asynchronous running of polymerase, at present, it is not possible to identify the sequence of the bases in a nucleic acid strand using this method (Figure 2d). It should be highlighted that this system provides solutions to two crucial obstacles in nanopore-based DNA sequencing: translocation control by polymerase, and nearly single-nucleotide resolution through MspA. Recently developed DNA-origami techniques offer an inspiration for customizing the shape and surface functionality of nanopores with near-atomic precision. As shown in Figure 2e, a nanometer-scale transmembrane channel that mimics the structure of αHL has been created by the self-assembly of DNA and DNA-bound cholesterol moieties.[27] This DNA-origami nanopore has a central opening with a diameter of 2 nm and could be inserted into the bilayer. Another well-designed DNA origami displays the possibility of hybridization with a solid-state nanopore (Figure 2f).[28] These origami nanopores have the ability to detect single DNA molecules and thus the potential to be applied in DNA sequencing. Furthermore, the development of other self-assembly nanomaterials will promote the design of sophisticated nanopores for DNA sequencing,[30] because their tunable geometry at nanoscale precision and specific modification would provide distinguished signals.

2.2. Conformation-Based Detection of Nucleic Acids by αHL Nanopores

Although nucleic acids can enter the wide vestibule of αHL in different conformations, only ssDNA in an extended conformation can translocate through the constriction. A polynucleotide (or its complex) undergoes conformational changes, such as unzipping and unfolding processes, in the vestibule of αHL to reduce the energy barrier for the successive translocation in its single-stranded and extended form. This property considerably intrigued researchers who employed αHL for the sensitive and specific sensing at single-molecule level.

In 1999, Akeson and co-workers demonstrated that αHL nanopore could rapidly discriminate individual polynucleotides because of their specific conformations. They showed that poly(A) produces a larger blockade current than poly(C) and poly(U) because of the helical structure of poly(A).[11] Meanwhile, Kasianowicz and co-workers showed that a freely jointed chain of poly(dT) induced a distinct double-step blockade current compared to that of the rigid secondary structure of poly(dC) and poly(dA), which produced pulse-like signals.[25a,31] An antigen-binding fragment, Fab HED10, acting as a rudder, forced poly(dT) into an extended conformation and decreased the energy barrier significantly (Figure 3a).[32] Moreover, an αHL nanopore was utilized to study the folded and unfolded states of an aptamer whose conformation is the key to the specific binding of a target molecule.[33] The G-quadruplex structure of the aptamer undergoes an unfolding process in the vestibule of αHL, resulting in a distinguishable blockade current.[33a] The real-time monitoring of the molecular conformational changes of the ATP-binding aptamer, occurring by binding targets, was further achieved (Figure 3b).[33b] Thus, the signatures of target-bound conformations of aptamers provide a rapid method for the specific sensing. For example, the detection of 300 ng mL^{-1} cocaine could be completed within 60 s by recognizing the capturing events of cocaine-aptamer with cocaine.[33c] To improve the detection efficiency for native bases of DNA, biotinylated ssDNA strands were captured and immobilized in an αHL nanopore by directly binding to avidin/streptavidin. Because the attached protein is too large to pass through the αHL, it causes a longer residence time of an ssDNA strand within the αHL (Figure 3c). This strategy enables the discrimination between single-base substitution,[21,22,34] an epigenetic DNA modification,[35] a single oxidative base lesion,[36] and abasic segments.[37]

Once captured by the αHL nanopore, double-stranded (dsDNA) with leader sequences unzips in the vestibule of the αHL nanopore under an applied potential.[38] The completion of the unzipping process takes significantly longer for ssDNA hybridized to the perfect complementary strand than for the same ssDNA hybridized to a sequence with single-nucleotide mismatch.[38a] Therefore, this strategy was successfully used to probe for single-nucleotide mismatches. By studying the unzipping kinetics of oxidatively damaged dsDNA, a single site of oxidized lesions could be identified in a sequence-specific location.[38c,f] To analyze microRNA in plasma samples from lung patients, a target microRNA was hybrid-

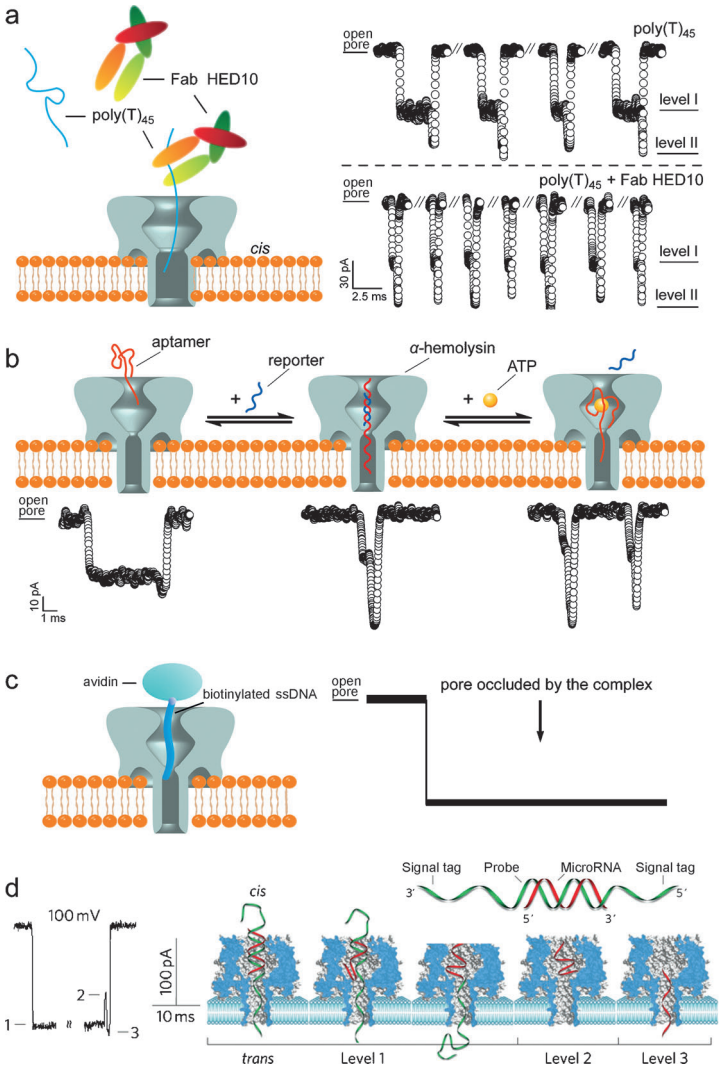

Figure 3. Conformation-based detection of nucleic acids using an αHL pore. a) Translocation time of poly(dT)$_{45}$ through an αHL pore was reduced in the presence of Fab HED10.[32] b) The αHL pore allows the detection of an ATP-binding aptamer in its folded, linear duplex strand and ATP-bound conformations.[33b] c) After binding to avidin, biotinylated ssDNA occluded the αHL pore, generating a long-time blockade. d) A typical multi-level signal produced by the translocation of unzipped microRNA through αHL.[38d] Reproduced with permission from Ref. [32, 33b, 38d].

ized with a ssDNA probe with leader sequences at both ends (Figure 3d).[38d] By monitoring the specific signatures, it was possible to quantify subpicomolar levels of cancer-associated microRNAs with αHL nanopores. Besides, the unzipping process of a hairpin structure was also adopted in mercury (Hg^{2+}) detection with the detection limit of 7 nM.[38e]

3. Solid-State Nanopores

3.1. DNA Detection with Solid-State Nanopores

The first synthetic solid-state nanopore that was successfully used for DNA sensing was developed by Li et al.,[39] who drilled the nanopore into an SiN layer using an ion beam. They tested the ability of these synthetic solid-state nanopores (diameter of 5 nm) to detect dsDNA molecules and detected a clear diminution of the ionic current when driving 500 bp dsDNA at an applied potential of 120 mV through the pore. When a voltage is applied, the electrical behavior of a nanopore with a diameter of 2–20 nm in an electrolyte solution roughly obeys Ohms low. A stable open pore current I_0 could be estimated by following equation:

$$I_0 = \frac{VA_\rho}{\rho H_{\text{eff}}} \quad (1)$$

Where ρ is the resistivity of the electrolyte solution, V is the applied voltage across the membrane, H_{eff} is the effective membrane thickness, and A_ρ is the mean cross-section area of a nanopore.[9d]

Although solid-state nanopores offer stability, durability, and other advantages, fabricated nanopores also have uncharacterized and possibly unfavorable surface properties that might greatly influence the sensing abilities of the pore. Compared to the biological nanopores, high electrical noise in solid-state nanopores results in a lower resolution. Previous studies[40] demonstrated that flicker noise ($1/f$) in solid-state nanopores originates from charge fluctuations at the nanopore surface, fluctuations in the total number of charge carriers, and nanometer-sized gaseous bubbles inside the pore. Fine-tuning the surface properties of SiN nanopores by atomic-layer deposition (ALD) of alumina could significantly reduce $1/f$ noise.[41] Furthermore, Al_2O_3 nanopores show reduced high-frequency noise, high signal-to-noise ratio, and enhanced sensitivity during DNA translocation experiments.[42] Treatment of a silicon support chip with piranha solution would also reduce $1/f$ noise.[40e] In addition, the nanobubbles can be removed by exchanging the solution with water and then ethanol before changing back to the measurement buffer.[40d]

One of the remaining challenges of using solid-state nanopores in DNA sequencing is the high translocation velocity, which causes difficulties in reading the sequencing information from the current signatures.[9c] Bashir and co-workers reported reduced translocation rates in Al_2O_3 pores because of their unique ability to form positively charged crystal domains during sputtering.[42b] Dekker and co-workers changed the anion of the buffer solution and found that the translocation time of a dsDNA/ssDNA molecule through a solid-state nanopore strongly increased as the counterions decreased in size from K^+ to Na^+ to Li^+.[43] The nanometer-scale thickness of a solid membrane fabricated by a traditional process impedes the direct application of introduced solid-state nanopores in DNA sequencing with single-base resolution. For example, an approximately 30 nm thick silicon-based membrane corresponds to around 60 bases along an ssDNA molecule. Graphene quickly attracted the attention of scientists because of its extraordinary thinness (0.34–0.68 nm), which is com-

parable to the spacing between adjacent nucleotides in ssDNA (0.32–0.52 nm).[44] The first single nanopore in suspended graphene was fabricated by Fischbein and Drndic.[45] Later, individual dsDNA molecules were driven through graphene nanopores (Figure 4a,b),[46] and translocation signals of DNA were obtained, thus confirming the great potential of graphene nanopores in DNA sequencing. The high $1/f$ noise in graphene nanopores prohibited the direct detection of individual nucleotides by reading the ionic current. Studies showed that multilayered graphene/Al_2O_3 nanolaminate membranes exhibited a lower electrical noise than nanopores in pure graphene.[44] Nevertheless, many issues, including the resolution of single bases, need to be addressed before graphene nanopores can be utilized in DNA sequencing.

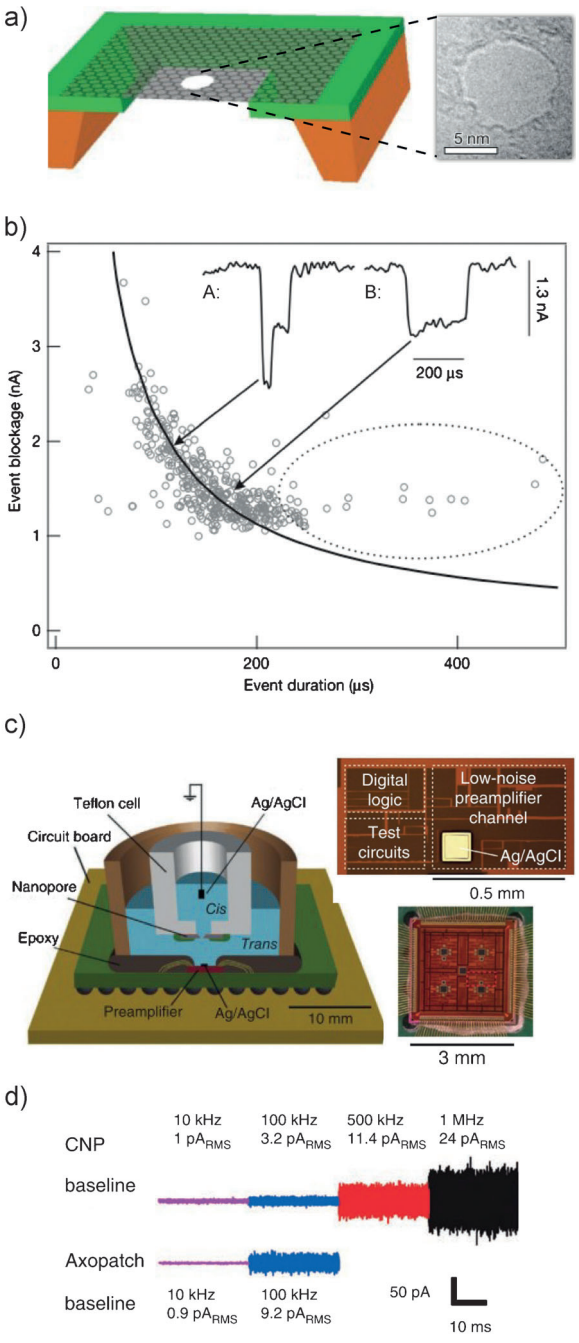

Figure 4. a) Diagram and TEM image of a thin sheet of graphene nanopores.[45a] b) Scatter plots of blockade current versus blockade duration illustrating the discrimination of folded (A) and unfolded (B) DNA.[45a] c) Schematic of CNP (left), a preamplifier channel (right, top), and an 8-channel CMOS voltage–clamp current preamplifier (right, bottom).[8b] d) Baseline noise for CNP and Axopatch 200B.[8b] Reproduced with permission from Ref. [8b] and [45a].

3.2. Platforms for Electrochemical Detection

A traditional platform for nanopore-based detection consists of a patch–clamp amplifier and an analog–digital converter. Axopatch 200B, the patch-clamp amplifier that shows the best performance in nanopore experiments, has a temporal resolution of around 4 µs. However, at present, the solid-state nanopore performs with a high DNA translocation velocity (1—100 nucleotides/ms^{-1}), which pushes the detector bandwidth requirements to the MHz region and precludes the measurement of pico-ampere steps in ionic current. The traditonal patch–clamp system has to be constrained to the bandwidth below around 100 kHz because the high frequency ($\geq$ 10 kHz) will result in high noise level in the measurements, mainly from the amplifier and the sum of various capacitances. Therefore, the way to achieve a high time resolution together with a low noise needs to be considered carefully. A recently reported complementary metal oxide semiconductor (CMOS) integrated nanopore platform (CNP), which consists of a custom-designed low-noise current preamplifier and an SiN solid-state nanopore, works at a bandwidth of 1 MHz at a noise level of 24 pA$_{RMS}$ (Figure 4c).[8b] This platform exhibits the highest bandwidth known to date for nanopore recording. The amplifier is directly positioned inside the fluid chamber with the SiN pores above the amplifier. This design considerably reduced parasitic capacitances at high frequency. For example, the CNP has a noise floor of 3.2 pA$_{RMS}$ at 100 kHz, compared to 9 pA$_{RMS}$ for the Axopatch (Figure 4d).

To meet the requirement of rapid high-throughput DNA sequencing, the fabrication of nanopore-based platforms in multichannel nanopore-based arrays is of the greatest interest. The design of a planar amplifier of the CNP is suitable for the parallelization, and supports the portability of multichannel detection.[8b] Besides, a pseudo-resistor that uses a deep N-well NMOS has been developed by Dunbar et al., aiming at reducing the feedback resistor size for the nanopore arrays.[47] This whole platform for detection was fabricated in a 0.35 µm CMOS process. As estimated,[48] 1500 channels could be integrated into a die with a size of 600 mm^2 if the realistic CMOS amplifier including the contact pat takes an area of 0.4 mm^2. Therefore, a portable nanopore array with high temporal resolution and low noise can be obtained. By combining novel detection platforms and experimental strategies, single-nucleotide resolution may eventually be achieved with solid-state nanopores.

4. Conclusions

Present DNA detection methods show the patterns of current levels related to known DNA strands,[3a] however, a big obstacle still hinders the application of nanopores in DNA sequencing with unknown sequences. Although presently nanopore sensors are not directly applicable in DNA sequencing, both biological and solid-state nanopores are excellent single-molecule sensors in biophysics and nanobiotechnology. The combination of solid-state nanopores with other single-molecule techniques provides a multimodal approach to detect small features along an individual DNA molecule. Integrating the advantages in experimental strategies of nanopores, microfabrication technologies, and the design of circuitry will accelerate nanopore technology toward affordable and personalized DNA detection, especially for DNA sequencing. Furthermore, we have no doubt that nanopore-based techniques will become routine analytical tool in single-molecule studies or even in medical detection.

The authors acknowledge funding of the National Base Research 973 Program (2013CB733700). Y.-T.L. is grateful for funds from the National Science Fund of China (21125522, 21327807, and SKLEAC201305). Y.-L.Y. thanks the Sino-UK Higher Education Research Partnership for PhD Studies.

Received: April 25, 2013
Published online: November 8, 2013

[1] a) J. Kasianowicz, E. Brandin, D. Branton, D. Deamer, *Proc. Natl. Acad. Sci. USA* **1996**, *93*, 13770 – 13773; b) L. Song, M. R. Hobaugh, C. Shustak, S. Cheley, H. Bayley, J. E. Gouaux, *Science* **1996**, *274*, 1859 – 1866.

[2] a) R. Stefureac, Y. Long, H. B. Kraatz, P. Howard, J. S. Lee, *Biochemistry* **2006**, *45*, 9172 – 9179; b) M. Pastoriza-Gallego, L. Rabah, G. Gibrat, B. Thiebot, F. G. van der Goot, L. Auvray, J.-M. Betton, J. Pelta, *J. Am. Chem. Soc.* **2011**, *133*, 2923 – 2931.

[3] a) E. A. Manrao, I. M. Derrington, A. H. Laszlo, K. W. Langford, M. K. Hopper, N. Gillgren, M. Pavlenok, M. Niederweis, J. H. Gundlach, *Nat. Biotechnol.* **2012**, *30*, 349 – 353; b) T. Z. Butler, M. Pavlenok, I. M. Derrington, M. Niederweis, J. H. Gundlach, *Proc. Natl. Acad. Sci. USA* **2008**, *105*, 20647 – 20652.

[4] M. Soskine, A. Biesemans, B. Moeyaert, S. Cheley, H. Bayley, G. Maglia, *Nano Lett.* **2012**, *12*, 4895 – 4900.

[5] M. M. Mohammad, R. Iyer, K. R. Howard, M. P. McPike, P. N. Borer, L. Movileanu, *J. Am. Chem. Soc.* **2012**, *134*, 9521 – 9531.

[6] a) D. Wendell, P. Jing, J. Geng, V. Subramaniam, T. J. Lee, C. Montemagno, P. Guo, *Nat. Nanotechnol.* **2009**, *4*, 765 – 772; b) F. Haque, J. Geng, C. Montemagno, P. Guo, *Nat. Protoc.* **2013**, *8*, 373 – 392.

[7] H. Y. Wang, Y. Li, L. X. Qin, A. Heyman, O. Shoseyov, I. Willner, Y. T. Long, H. Tian, *Chem. Commun.* **2013**, *49*, 1741 – 1743.

[8] a) U. Keyser, J. Van der Does, C. Dekker, N. Dekker, *Rev. Sci. Instrum.* **2006**, *77*, 105105; b) J. K. Rosenstein, M. Wanunu, C. A. Merchant, M. Drndic, K. L. Shepard, *Nat. Methods* **2012**, *9*, 487 – 492; c) B. McNally, A. Singer, Z. Yu, Y. Sun, Z. Weng, A. Meller, *Nano Lett.* **2010**, *10*, 2237 – 2244.

[9] a) B. N. Miles, A. P. Ivanov, K. A. Wilson, F. Doğan, D. Japrung, J. B. Edel, *Chem. Soc. Rev.* **2013**, *42*, 15 – 28; b) J. E. Reiner, A. Balijepalli, J. W. Robertson, J. Campbell, J. Suehle, J. J. Kasianowicz, *Chem. Rev.* **2012**, *112*, 6431 – 6451; c) B. M. Venkatesan, R. Bashir, *Nat. Nanotechnol.* **2011**, *6*, 615 – 624; d) J. Li, J. A. Golovchenko in *Methods in Molecular Biology, Vol. 544* (Eds.: J. W. Lee, R. S. Foote), Humana Press, **2009**, pp. 81 – 93.

[10] D. Branton, D. W. Deamer, A. Marziali, H. Bayley, S. A. Benner, T. Butler, M. Di Ventra, S. Garaj, A. Hibbs, X. Huang, *Nat. Biotechnol.* **2008**, *26*, 1146 – 1153.

[11] M. Akeson, D. Branton, J. J. Kasianowicz, E. Brandin, D. Deamer, *Biophys. J.* **1999**, *77*, 3227 – 3233.

[12] R. Kawano, A. E. P. Schibel, C. Cauley, H. S. White, *Langmuir* **2009**, *25*, 1233 – 1237.

[13] A. Meller, L. Nivon, E. Brandin, J. Golovchenko, D. Branton, *Proc. Natl. Acad. Sci. USA* **2000**, *97*, 1079 – 1084.

[14] M. Rincon-Restrepo, E. Mikhailova, H. Bayley, G. Maglia, *Nano Lett.* **2011**, *11*, 746 – 750.

[15] L. Blanco, A. Bernad, J. M. Lázaro, G. Martin, C. Garmendia, M. Salas, *J. Biol. Chem.* **1989**, *264*, 8935 – 8940.

[16] a) N. Hurt, H. Wang, M. Akeson, K. R. Lieberman, *J. Am. Chem. Soc.* **2009**, *131*, 3772-3778; b) B. Gyarfas, F. Olasagasti, S. Benner, D. Garalde, K. R. Lieberman, M. Akeson, *ACS Nano* **2009**, *3*, 1457 – 1466.

[17] K. R. Lieberman, G. M. Cherf, M. J. Doody, F. Olasagasti, Y. Kolodji, M. Akeson, *J. Am. Chem. Soc.* **2010**, *132*, 17961 – 17972.

[18] G. M. Cherf, K. R. Lieberman, H. Rashid, C. E. Lam, K. Karplus, M. Akeson, *Nat. Biotechnol.* **2012**, *30*, 344 – 348.

[19] F. Olasagasti, K. R. Lieberman, S. Benner, G. M. Cherf, J. M. Dahl, D. W. Deamer, M. Akeson, *Nat. Nanotechnol.* **2010**, *5*, 798 – 806.

[20] S. Kumar, C. Tao, M. Chien, B. Hellner, A. Balijepalli, J. W. Robertson, Z. Li, J. J. Russo, J. E. Reiner, J. J. Kasianowicz, J. Ju, *Sci. Rep.* **2012**, *2*, 684.

[21] D. Stoddart, A. J. Heron, E. Mikhailova, G. Maglia, H. Bayley, *Proc. Natl. Acad. Sci. USA* **2009**, *106*, 7702 – 7707.

[22] D. Stoddart, G. Maglia, E. Mikhailova, A. J. Heron, H. Bayley, *Angew. Chem.* **2010**, *122*, 566 – 569; *Angew. Chem. Int. Ed.* **2010**, *49*, 556 – 559.

[23] L. Q. Gu, O. Braha, S. Conlan, S. Cheley, H. Bayley, *Nature* **1999**, *398*, 686 – 690.

[24] J. Clarke, H. C. Wu, L. Jayasinghe, A. Patel, S. Reid, H. Bayley, *Nat. Nanotechnol.* **2009**, *4*, 265 – 270.

[25] a) S. E. Henrickson, M. Misakian, B. Robertson, J. J. Kasianowicz, *Phys. Rev. Lett.* **2000**, *85*, 3057 – 3060; b) T. Z. Butler, J. H. Gundlach, M. Troll, *Biophys. J.* **2007**, *93*, 3229 – 3240.

[26] E. Pennisi, *Science* **2012**, *336*, 534 – 537.

[27] M. Langecker, V. Arnaut, T. G. Martin, J. List, S. Renner, M. Mayer, H. Dietz, F. C. Simmel, *Science* **2012**, *338*, 932 – 936.

[28] N. A. Bell, C. R. Engst, M. Ablay, G. Divitini, C. Ducati, T. Liedl, U. F. Keyser, *Nano Lett.* **2012**, *12*, 512 – 517.

[29] I. M. Derrington, T. Z. Butler, M. D. Collins, E. Manrao, M. Pavlenok, M. Niederweis, J. H. Gundlach, *Proc. Natl. Acad. Sci. USA* **2010**, *107*, 16060 – 16065.

[30] a) M. D. Ward, P. R. Raithby, *Chem. Soc. Rev.* **2013**, *42*, 1619 – 1636; b) R. Shenhar, T. B. Norsten, V. M. Rotello, *Adv. Mater.* **2005**, *17*, 657 – 669; c) O. Wilner, I. Willner, *Chem. Rev.* **2012**, *112*, 2528 – 2556.

[31] J. J. Kasianowicz, S. E. Henrickson, H. H. Weetall, B. Robertson, *Anal. Chem.* **2001**, *73*, 2268 – 2272.

[32] Y. L. Ying, D. W. Li, Y. Li, J. S. Lee, Y.-T. Long, *Chem. Commun.* **2011**, *47*, 5690 – 5692.

[33] a) J. W. Shim, L. Q. Gu, *J. Phys. Chem. B* **2008**, *112*, 8354 – 8360; b) Y. L. Ying, H. Y. Wang, T. C. Sutherland, Y. T. Long, *Small* **2011**, *7*, 87 – 94; c) R. Kawano, T. Osaki, H. Sasaki, M. Takinoue, S. Yoshizawa, S. Takeuchi, *J. Am. Chem. Soc.* **2011**, *133*, 8474 – 8477.

[34] R. F. Purnell, J. J. Schmidt, *ACS Nano* **2009**, *3*, 2533 – 2538.

[35] E. V. Wallace, D. Stoddart, A. J. Heron, E. Mikhailova, G. Maglia, T. J. Donohoe, H. Bayley, *Chem. Commun.* **2010**, *46*, 8195 – 8197.

[36] A. E. Schibel, N. An, Q. Jin, A. M. Fleming, C. J. Burrows, H. S. White, *J. Am. Chem. Soc.* **2010**, *132*, 17992 – 17995.

[37] N. An, A. M. Fleming, H. S. White, C. J. Burrows, *Proc. Natl. Acad. Sci. USA* **2012**, *109*, 11504 – 11509.

[38] a) A. F. Sauer-Budge, J. A. Nyamwanda, D. K. Lubensky, D. Branton, *Phys. Rev. Lett.* **2003**, *90*, 238101; b) T. C. Sutherland, M. J. Dinsmore, H. B. Kraatz, J. S. Lee, *Biochem. Cell Biol.* **2004**, *82*, 407 – 412; c) A. E. P. Schibel, A. M. Fleming, Q. Jin, N. An, J. Liu, C. P. Blakemore, H. S. White, C. J. Burrows, *J. Am. Chem. Soc.* **2011**, *133*, 14778 – 14784; d) Y. Wang, D. Zheng, Q. Tan, M. X. Wang, L. Q. Gu, *Nat. Nanotechnol.* **2011**, *6*, 668 – 674; e) S. Wen, T. Zeng, L. Liu, K. Zhao, Y. Zhao, X. Liu, H. C. Wu, *J. Am. Chem. Soc.* **2011**, *133*, 18312 – 18317; f) Q. Jin, A. M. Fleming, C. J. Burrows, H. S. White, *J. Am. Chem. Soc.* **2012**, *134*, 11006 – 11011; g) K. Tian, Z. He, Y. Wang, S.-J. Chen, L.-Q. Gu, *ACS Nano* **2013**, *7*, 3962 – 3969.

[39] J. Li, D. Stein, C. McMullan, D. Branton, M. Aziz, J. Golovchenko, *Nature* **2001**, *412*, 166 – 169.

[40] a) D. P. Hoogerheide, S. Garaj, J. A. Golovchenko, *Phys. Rev. Lett.* **2009**, *102*, 256804; b) R. Smeets, N. Dekker, C. Dekker, *Nanotechnology* **2009**, *20*, 095501; c) R. M. M. Smeets, U. F. Keyser, N. H. Dekker, C. Dekker, *Proc. Natl. Acad. Sci. USA* **2008**, *105*, 417; d) R. Smeets, U. Keyser, M. Wu, N. Dekker, C. Dekker, *Phys. Rev. Lett.* **2006**, *97*, 88101; e) V. Tabard-Cossa, D. Trivedi, M. Wiggin, N. N. Jetha, A. Marziali, *Nanotechnology* **2007**, *18*, 305505.

[41] a) P. Chen, T. Mitsui, D. B. Farmer, J. Golovchenko, R. G. Gordon, D. Branton, *Nano Lett.* **2004**, *4*, 1333 – 1337; b) P. Chen, J. Gu, E. Brandin, Y. R. Kim, Q. Wang, D. Branton, *Nano Lett.* **2004**, *4*, 2293 – 2298.

[42] a) B. M. Venkatesan, B. Dorvel, S. Yemenicioglu, N. Watkins, I. Petrov, R. Bashir, *Adv. Mater.* **2009**, *21*, 2771 – 2776; b) B. M. Venkatesan, A. B. Shah, J. M. Zuo, R. Bashir, *Adv. Funct. Mater.* **2010**, *20*, 1266 – 1275.

[43] S. W. Kowalczyk, D. B. Wells, A. Aksimentiev, C. Dekker, *Nano Lett.* **2012**, *12*, 1038 – 1044.

[44] B. M. Venkatesan, D. Estrada, S. Banerjee, X. Jin, V. E. Dorgan, M. H. Bae, N. R. Aluru, E. Pop, R. Bashir, *ACS Nano* **2012**, 6, 441 – 450.

[45] M. D. Fischbein, M. Drndic, *Appl. Phys. Lett.* **2008**, *93*, 113107.

[46] a) S. Garaj, W. Hubbard, A. Reina, J. Kong, D. Branton, J. Golovchenko, *Nature* **2010**, *467*, 190 – 193; b) C. A. Merchant, K. Healy, M. Wanunu, V. Ray, N. Peterman, J. Bartel, M. D. Fischbein, K. Venta, Z. Luo, A. C. Johnson, *Nano Lett.* **2010**, *10*, 2915 – 2921.

[47] J. Kim, K. Pedrotti, W. B. Dunbar, *Sens. Actuators B* **2013**, *176*, 1051 – 1055.

[48] R. D. Maitra, J. Kim, W. B. Dunbar, *Electrophoresis* **2012**, *33*, 1 – 11.